

Effects of the Ancillary Ligands on Palladium–Carbon Bonding in (η^3 -Allyl)palladium Complexes. Implications for Nucleophilic Attack at the Allylic Carbons

Kálmán J. Szabó

Department of Organic Chemistry, University of Uppsala, Box 531, S-751 21 Uppsala, Sweden

Received September 7, 1995[Ⓢ]

[(η^3 -allyl)Pd]⁺ (**1**) and (η^3 -allyl)PdL₂ (L = F⁻, Cl⁻, NH₃, CH₂=CH₂ and PH₃) species (**2–6**) have been studied at the second-order Møller–Plesset (MP2) and fourth order Møller–Plesset (MP4) perturbation theory levels, the latter including single, double, and quadruple excitations (MP4SDQ). The nature of palladium–carbon interactions has been investigated on the basis of calculated electron density and energy density distributions. Complexation of **1** with σ -donors (F⁻, Cl⁻, NH₃) strengthens the palladium–carbon bonds and weakens the carbon–carbon bonds of the allyl moiety. This effect is more pronounced for F⁻ than Cl⁻ or NH₃ ligands. In contrast to σ -donors, π -acceptors significantly weaken the interactions between the palladium and η^3 -allyl groups. On the basis of the computational results, expected ligand effects on the reactivity and regioselectivity in nucleophilic additions are also discussed.

1. Introduction

Palladium-catalyzed allylic substitution^{1–4} and 1,4-oxidation of conjugate dienes^{5–7} have recently been the subject of great interest from organic chemists due to their wide synthetic scope, practical simplicity, and potential for regio- and stereoselective synthesis. (η^3 -allyl)Pd^{II} complexes, the key intermediates in these reactions, have been studied extensively because of the extremely useful reactions of nucleophiles with the allylic moiety. Åkermark,^{8–10} Hoffmann,^{11–13} and Bäckvall,¹⁴ and their co-workers have demonstrated that the nature of the ancillary ligand (L) employed in the palladium-catalyzed substitutions and 1,4-oxidations has a significant effect on the rate of reaction and also on the control of the regioselectivity of the reaction. Importance of the ligand effects on the stereochemical outcome of the nucleophilic attack is discussed in a number of synthetic and mechanistic studies by Bosnich,^{15,16} Hayashi,^{17,18} Trost¹⁹ and others.^{20–22} It was shown, for example, that the reaction is greatly acceler-

ated in the presence of π -accepting ligands, such as phosphines, but not by ligands which are only able to function as σ -donors. On the other hand, π -acceptors induce nucleophilic attack at the terminal carbons (C₁) of the η^3 -allyl moiety, while use of certain σ -donors such as tmeda directs the nucleophile attack to the central carbon (C₂).^{11–13,23} Effects of the allylic functional groups on the regio- and stereoselectivity also depend on the nature of ligands employed in the reaction,^{7–10,24,25} indicating that the electronic effects of the ligands are transmitted to further parts of the allylic moiety.

Theoretical aspects of the metal–ligand bonding in the Ni, Pd, Pt triad were systematically investigated by Siegbahn,^{26–29} Goddard,^{30–34} and their co-workers. However, high-level ab initio data on Ni and Pd allyl

(15) Auburn, P. R.; Mackenzie, P. B.; Bosnich, B. *J. Am. Chem. Soc.* **1985**, *107*, 2033.

(16) Mackenzie, P. B.; Whelan, J.; Bosnich, B. *J. Am. Chem. Soc.* **1985**, *107*, 2046.

(17) Hayashi, T.; Hagira, T.; Konishi, M.; Kumada, M. *J. Am. Chem. Soc.* **1983**, *105*, 7767.

(18) Hayashi, T.; Konishi, M.; Kumada, M. *J. Chem. Soc., Chem. Commun.* **1984**, 107.

(19) Trost, B. M.; Murphy, D. J. *Organometallics* **1985**, *4*, 1143.

(20) Pfaltz, A. *Acc. Chem. Res.* **1993**, *26*, 339.

(21) Brencley, G.; Merifield, E.; Wills, M.; Fedouloff, M. *Tetrahedron Lett.* **1994**, *35*, 2791.

(22) Anderson, P. G.; Harden, A.; Tanner, D.; Norrby, P.-O. *Chem. Eur.* **1995**, *1*, 12.

(23) Castaño, A. M.; Aranyos, A.; Szabó, K. J.; Bäckvall, J.-E. *Angew. Chem., Int. Ed. Engl.* **1995**, *34*, 2551.

(24) Bäckvall, J.-E.; Nyström, J.-E.; Nordberg, R. E. *J. Am. Chem. Soc.* **1985**, *107*, 3676.

(25) Andersson, P. G.; Aranyos, A. *Tetrahedron Lett.* **1994**, *35*, 4441.

(26) Siegbahn, P. E. M. *J. Am. Chem. Soc.* **1994**, *116*, 7722.

(27) Siegbahn, P. E. M. *Theor. Chim. Acta* **1994**, *87*, 441.

(28) Siegbahn, P. E. M. *J. Am. Chem. Soc.* **1993**, *115*, 5803.

(29) Siegbahn, P. E. M.; Svensson, M. *Chem. Phys. Lett.* **1993**, *216*, 147.

(30) Irikura, K. K.; Goddard, W. A., III. *J. Am. Chem. Soc.* **1994**, *116*, 8733.

(31) Ohanessian, G.; Goddard, W. A., III. *Acc. Chem. Res.* **1990**, *23*, 386.

(32) Carter, E. A.; Goddard, W. A., III. *J. Phys. Chem.* **1988**, *92*, 5679.

(33) Schilling, J. B.; Goddard, W. A., III; Beauchamp, J. L. *J. Am. Chem. Soc.* **1987**, *109*, 5573.

(34) Schilling, J. B.; Goddard, W. A., III; Beauchamp, J. L. *J. Am. Chem. Soc.* **1987**, *109*, 5566.

[Ⓢ] Abstract published in *Advance ACS Abstracts*, January 15, 1996.

(1) Heumann, A.; Réglér, M. *Tetrahedron* **1995**, *51*, 975.

(2) Frost, C. G.; Howarth, J.; Williams, J. M. J. *Tetrahedron: Asymmetry* **1992**, *3*, 1089.

(3) Godleski, S. A. *Comprehensive Organic Synthesis*; Pergamon Press: New York, 1991; Vol. 4, p 585.

(4) Trost, B. M. *Acc. Chem. Res.* **1980**, *13*, 385.

(5) Bäckvall, J.-E. *Pure Appl. Chem.* **1992**, *64*, 429.

(6) Bäckvall, J.-E. *Acc. Chem. Res.* **1983**, *16*, 335.

(7) Bäckvall, J.-E.; Byström, S. E.; Nordberg, R. E. *J. Org. Chem.* **1984**, *49*, 4619.

(8) Åkermark, B.; Zetterberg, K.; Hansson, S.; Krakenberger, B.; Vitagliano, A. *J. Organomet. Chem.* **1987**, *335*, 133.

(9) Åkermark, B.; Hansson, S.; Krakenberger, B.; Vitagliano, A.; Zetterberg, K. *Organometallics* **1984**, *3*, 679.

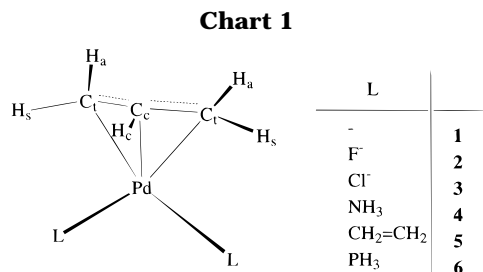
(10) Åkermark, B.; Krakenberger, B.; Hansson, S.; Vitagliano, A. *Organometallics* **1987**, *6*, 620.

(11) Hoffmann, H. M. R.; Otte, A. R.; Wilde, A.; Menzer, S.; Williams, D. J. *Angew. Chem., Int. Ed. Engl.* **1995**, *34*, 100.

(12) Otte, A. R.; Wilde, A.; Hoffmann, H. M. R. *Angew. Chem., Int. Ed. Engl.* **1994**, *33*, 1280.

(13) Wilde, A.; Otte, A. R.; Hoffmann, H. M. R. *J. Chem. Soc., Chem. Commun.* **1993**, 615.

(14) Castaño, A. M.; Bäckvall, J.-E. *J. Am. Chem. Soc.* **1995**, *117*, 560.



complexes are rather scarce: Goddard and co-workers³⁵ studied the structure of bis(η^3 -allyl)nickel at the Hartree–Fock (HF) level of theory, and Norrby and co-workers³⁶ calculated the geometry of [$(\eta^3$ -allyl)Pd]⁺ (**1**) using the modified coupled pair functional (MCPF) method. Most of the theoretical calculations on (η^3 -allyl)PdL₂ and related complexes have been carried out on a semiempirical level.^{37–40} Although the EHMO studies by Nakasuji,³⁹ Eisenstein,³⁸ and Mealli⁴⁰ disclosed many important structural features of the (η^3 -allyl)PdL₂ complexes, a number of questions, concerning for example the effects of the ancillary ligands on the geometry, electron distribution, and thermodynamic stability, are not clear. In this work, the following questions will be discussed.

(1) How do σ -donor and π -acceptor ligands influence the palladium–carbon bond lengths and the overall stability of the complex?

(2) What is the relationship between the σ -donor ability and electronegativity of the ligand?

(3) What is the character of the palladium–carbon bonds?

(4) How does the electron density in the palladium–carbon internuclear region depend on the nature of the ancillary ligand?

(5) How are the π -acceptor effects of the ligands transmitted to the allyl moiety? Why do π -acceptors activate the (η^3 -allyl)Pd complexes toward nucleophilic attack?

In order to answer these questions, ab initio calculations were carried out for simple model systems **1–6** (Chart 1), in which L groups (F⁻, Cl⁻, NH₃, CH₂=CH₂, PH₃) have the basic electronic effects of those ancillary ligands that are usually employed in allylic substitution and 1,4-oxidation reactions. Complex **1** is our reference system but can also be considered as a model for (η^3 -allyl)PdL₂ complexes with ancillary ligands of very low coordinating ability such as solvent molecules. In section 4 of this study the calculational results will be interpreted by means of a qualitative MO diagram. By this interpretation, certain properties such as structural parameters and reactivity of large, practically important (η^3 -allyl)PdL₂ complexes can also be predicted.

2. Computational Methods

The geometries of **1–6** were fully optimized by employing second-order Møller–Plesset (MP2) perturbation theory⁴¹ with-

(35) Goddard, R.; Krüger, C.; Mark, F.; Stansfield, R.; Zhang, X. *Organometallics* **1985**, *4*, 285.

(36) Norrby, P.-O.; Åkermark, B.; Häfner, F.; Hansson, S.; Blomberg, M. *J. Am. Chem. Soc.* **1993**, *115*, 4859.

(37) Sakaki, S.; Nishikawa, M.; Ohyoshi, A. *J. Am. Chem. Soc.* **1980**, *102*, 4062.

(38) Curtis, M. D.; Eisenstein, O. *Organometallics* **1984**, *3*, 887.

(39) Nakasuji, K.; Yamaguchi, M.; Murata, I.; Tatsumi, K.; Nakamura, A. *Organometallics* **1984**, *3*, 1257.

(40) Carfagna, C.; Galarini, R.; Linn, K.; López, J. A.; Mealli, C.; Musco, A. *Organometallics* **1993**, *12*, 3019.

out imposing any symmetry constraints. All electrons, for which the MOs are described by basis functions, were correlated. For hydrogens the primitive (4s)⁴² basis was used contracted to [2s]. For carbon, nitrogen, fluorine, phosphorus and chlorine atoms the (9s,5p) basis of Huzinaga⁴² was used, augmented with one d function⁴³ and contracted to [3s,2p,1d], with the phosphorus and chlorine core replaced by an ECP.⁴⁴ For fluorine and chlorine this basis set was augmented by one set of s and p diffuse functions. For palladium, a relativistic ECP according to Hay and Wadt⁴⁵ was used; the 4s and 4p orbitals were described by a single- ζ contraction; the valence 5s and 5p orbitals by a double- ζ basis and the 4d orbital by a triple- ζ basis that finally gave a LANL2DZ basis augmented with a diffuse d function. The whole basis set is referred to as basis set A.⁴⁶ Single-point calculations with MP2/A geometries have been carried out at a higher level of theory, namely at third-order MP (MP3) and fourth-order MP (MP4) where in the latter case single (S), double (D), and quadruple (Q) excitations have been included (MP4SDQ). In the single-point calculations the inner shells were excluded from the correlation energy calculations and basis set A was extended. For phosphorus and chlorine the (11s,7p,2d) [4s,3p,2d] basis set from Huzinaga^{43,47,48} was used and the basis set of palladium was augmented with a (3f) [1f] polarization function. This basis set is referred to as basis set B⁴⁹ and the single-point calculations are denoted by MP3/B//MP2/A and MP4SDQ/B//MP2/A.

In order to characterize the palladium–carbon bonds, MP2/A response densities were analyzed using the virial partitioning method of Bader and co-workers.⁵⁰ The calculated electron density distribution $\rho(\mathbf{r})$ and the energy density distribution $H(\mathbf{r})$ have been investigated in the way described by Cremer and Kraka.^{51,52} These authors have given two conditions for existence of a covalent bond in the internuclear region of two atoms A and B.

(1) Atoms A and B have to be connected by a path of maximum electron density (MED path). The existence of such a MED path implies a (3, -1) saddle point, the so-called bond critical point \mathbf{r}_b , of the electron density distribution $\rho(\mathbf{r})$ as well as a zero-flux surface between A and B (necessary condition).

(2) The local energy density $H(\mathbf{r}_b)$ has to be stabilizing; i.e., it must be smaller than zero (sufficient condition).

The bond critical points were evaluated by the density analysis program of Cremer and Kraka, while rest of the calculations have been performed with the GAUSSIAN92 program.⁵³

(41) Hariharan, P. C.; Pople, J. A. *Theor. Chim. Acta* **1973**, *28*, 213.

(42) Huzinaga, S. *J. Chem. Phys.* **1965**, *42*, 1293.

(43) Huzinaga, S.; Andzelm, J.; Klobukowski, M.; Radzio-Andzelm, E.; Sakai, Y.; Tatewaki, H. *Gaussian Basis Sets for Molecular Calculations*; Elsevier: Amsterdam, 1984.

(44) Hay, P. J.; Wadt, W. R. *J. Chem. Phys.* **1985**, *82*, 270.

(45) Hay, P. J.; Wadt, W. R. *J. Chem. Phys.* **1985**, *82*, 299.

(46) Exponents for the d functions: N, 0.864; C, 0.630; F, 1.496; P, 0.340; Cl, 0.514; Pd (diffuse d function), 0.0628. Exponents for the diffuse sp functions: F, 0.1076; Cl, 0.0483.

(47) Dunning, T. H.; Hay, P. J. *Modern Theoretical Chemistry*; Plenum Press: New York, 1977; Vol. 3.

(48) Petterson, L. G. M.; Siegbahn, P. E. M. *J. Chem. Phys.* **1985**, *83*, 3538.

(49) Exponents for the d functions: Cl, 0.95 and 0.32; P, 0.537 and 0.153; other d exponents are the same as in basis set A. Exponents and contraction coefficients for the f function of Pd are 3.612, 1.295, 0.555 and 0.174, 0.597, 0.393, respectively.

(50) Bader, R. F. W.; Nguyen-Dang, T. T. *Adv. Quantum Chem.* **1981**, *14*, 63.

(51) Kraka, K.; Cremer, D. In *The Concept of the Chemical Bond*; Maksic, Z. B., Ed.; Springer: Berlin, 1990; p 453.

(52) Cremer, D.; Kraka, E. *J. Am. Chem. Soc.* **1985**, *107*, 3800.

(53) Frisch, M. J.; Head-Gordon, M.; Trucks, G. W.; Foresman, J. B.; Schlegel, H. B.; Raghavachari, K.; Robb, M. A.; Binkley, J. S.; Gonzales, C.; Defrees, D. J.; Fox, D. J.; Whiteside, R. A.; Seeger, R.; Melius, C. F.; Baker, J.; Martin, R. L.; Kahn, L. R.; Stewart, J. J. P.; Topiol, S.; Popole, J. A. *Gaussian 92*; Gaussian Inc.: Pittsburgh, PA, 1992.

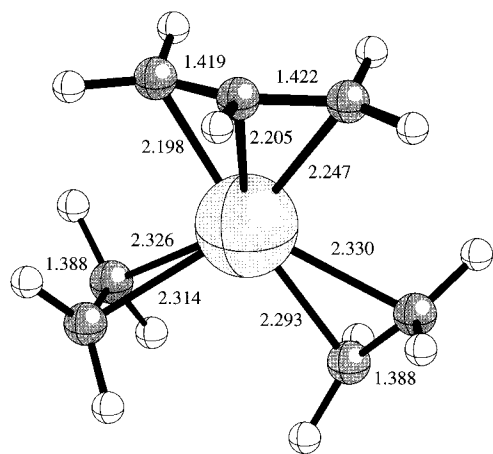


Figure 1. MP2/A geometry (bond lengths in Å) of $[(\eta^3\text{-allyl})\text{Pd}(\text{CH}_2=\text{CH}_2)_2]^+$ (**5**).

3. Results and Discussion

The MP2/A geometrical parameters of molecules **1–6** calculated in this work are summarized in Table 1. Complexation energies of **1** with F^- , Cl^- , NH_3 , $\text{CH}_2=\text{CH}_2$ and PH_3 are given in Table 2 (see also eq 1). In Tables 3 and 4 the Mulliken and bond density analysis of the MP2/A response density are given.

Geometry of the $(\eta^3\text{-allyl})\text{PdL}_2$ Complexes. The unconstrained MP2/A geometry optimization leads to C_s symmetrical structures **1–4** and **6**, as well as to structure **5** (Figure 1), which possesses C_1 symmetry. The lower symmetry of **5** is a consequence of the twisting of $\text{CH}_2=\text{CH}_2$ ligands. If **5** is forced to the C_s -symmetrical form, the shortest nonbonding distance between the hydrogens of the two ethylene ligands is 2.37 Å, which is shorter than the sum of the van der Waals radii of hydrogen atoms⁵⁴ (2.40 Å). However, when the symmetry constraint is released, the ethylene ligands move out of the C_s -symmetrical conformation, and as a consequence the shortest H–H nonbonding distance (2.54 Å) is increased by 0.17 Å, which relieves the nonbonding strain.

The equilibrium geometry calculated for **1** at the MP2/A level of theory is very similar to the data published by Norrby and co-workers.³⁶ These authors used the MCPF method in connection with a basis set of DZ+P quality. The Pd–C_t (2.16 Å) and Pd–C_c (2.15 Å) bond lengths at the MCPF level of theory are only slightly longer than at the MP2/A level (Pd–C_t = 2.17 Å, Pd–C_c = 2.16 Å). Similarity of the MP2 and MCPF geometries is in line with the observation of Siegbahn and Svensson.²⁹ According to these authors the MP2 geometrical parameters calculated for second-row transition-metal complexes are usually close to those obtained by using a higher level of theory such as QCISD and MCPF methods.

The experimental IR spectrum shows that **3** possesses C_s symmetry,⁵⁵ which is in agreement with the computational results. According to the available X-ray diffraction data, the Pd–C_t and Pd–C_c distances in $[(\eta^3\text{-allyl})\text{PdCl}]_2$ ⁵⁶ are 2.123(7) and 2.108(9) Å, respectively, while those in $[(\eta^3\text{-allyl})\text{PdCl}_2]^-$ ⁵⁷ are 2.14(2) and

2.09(3) Å, respectively, which agrees well with the calculated values of 2.123 and 2.075 Å (Table 1). In the X-ray diffraction structure of $[(\eta^3\text{-allyl})\text{Pd}(\text{tmeda})]^+$ ⁵⁷ Pd–C_t is 2.15(3) Å and Pd–C_c is 2.06(3) Å, which are close to the corresponding distances in **4** (Pd–C_t = 2.157 and Pd–C_c = 2.137 Å). The Pd–C_t distance trans to PPh_3 in the X-ray structure of $(\eta^3\text{-allyl})\text{Pd}(\text{PPh}_3)\text{Cl}$ ⁵⁸ is 2.211(6) Å which compares well with Pd–C_t = 2.212 Å in **6**.

Coordination of **1** with pure σ -donor ligands (F^- , Cl^- , NH_3) leads to shortening of Pd–C distances (Table 1). This effect depends on the σ -donor strength of the ligand: Pd–C distances are shorter by 0.07–0.10 Å in the fluoride complex **2** than in the NH_3 complex **4**. Comparing the Pd–C distances in the anionic species reveals that the more electronegative F^- (**2**) shortens Pd–C distances to a larger extent than does Cl^- (**3**). Since carbon and phosphorus are more electropositive than nitrogen, considering the trend found for fluoride and chloride ligands, somewhat longer Pd–C distances are expected in **5** and **6** than in **3**. However, in **5** and **6**, Pd–C distances are even longer than in the unligated complex **1**, which can be ascribed to the π -acceptor character of $\text{CH}_2=\text{CH}_2$ ^{59,60} and PH_3 ⁶¹ (*vide infra*). Small but significant changes can be observed for C_t–C_c distances and C_t–C_c–C_t angles of the allyl moiety. As one goes from **2** to **6**, C_t–C_c decreases from 1.44 to 1.42 Å, while C_t–C_c–C_t increases from 115 to 118°, gradually approaching the corresponding parameters in the free allyl species (C_t–C_c = 1.37–1.39 Å, C_t–C_c–C_t = 118–132°).^{62,63} A similar trend can be observed for displacement of C_tH₂ out of the CCC plane (Table 1, Figure 1). Deviation of the anti hydrogen (H_a) from the CCC plane is larger by 7° in **2** (38.5°) than in **6** (31.3°). On the basis of neutron diffraction data and HF/DZ calculations, Goddard and co-workers³⁵ report a similar distortion of the CH₂ groups (H_a–C_t–C_c–C_t = 31.4° (calculated), 29.9° (measured)) in the bis(η^3 -allyl)nickel complex. Distortion of the CH₂ units in free allyl species is energetically costly.⁶² However, as previously noted by Goddard and co-workers,³⁵ in allylmetal complexes this destabilization is compensated by (a) the improved overlap of the allylic π orbitals with the valence orbitals of the metal (b) a reduction in the repulsion between the metal atom and the anti hydrogen atoms (H_a).

Complexation Energies of 1. In the direct calculation of bond dissociation and complexation energies, Møller–Plesset perturbation theory frequently leads to oscillating values at different orders of perturbation theory.^{64–66} Hence, the MP n data should be used with a degree of caution when calculating energies of transition-metal complexes. However, it seems that quite reliable relative complexation energies can be obtained

(58) Faller, J. W.; Blankenship, C.; Whitmore, B.; Sena, S. *Inorg. Chem.* **1985**, *24*, 4483.

(59) Hay, J. F. *J. Am. Chem. Soc.* **1981**, *103*, 1390.

(60) Bäckvall, J.-E.; Björkman, E. E.; Pettersson, L.; Siegbahn, P. *J. Am. Chem. Soc.* **1984**, *106*, 4396.

(61) Marynick, D. S. *J. Am. Chem. Soc.* **1984**, *106*, 4064.

(62) Schleyer, P. v. R. *J. Am. Chem. Soc.* **1985**, *107*, 4793.

(63) Cometta-Morini, C.; Ha, T.-K.; Oth, J. F. M. *J. Mol. Struct. (Theochem)* **1989**, *188*, 79.

(64) Böhme, M.; Frenking, G. *Chem. Phys. Lett.* **1994**, *224*, 195.

(65) Neuhaus, A.; Frenking, G.; Huber, C.; Gauss, J. *Inorg. Chem.* **1992**, *31*, 5355.

(66) Jonas, V.; Frenking, G.; Gauss, J. *Chem. Phys. Lett.* **1992**, *194*, 109.

(54) Bondi, A. *J. Phys. Chem.* **1964**, *68*, 441.

(55) Goodfellow, R. J.; Venazi, L. M. *J. Chem. Soc. A* **1966**, 784.

(56) Smith, A. E. *Acta Crystallogr.* **1965**, *18*, 331.

(57) Hegedus, L. S.; Åkermark, B.; Olsen, D. J.; Anderson, O. P.; Zetterberg, K. *J. Am. Chem. Soc.* **1982**, *104*, 697.

Table 1. Selected Geometrical Parameters of Molecules 1–6^a

	sym	L	Pd–C _t	Pd–C _c	C _c –C _t	Pd–L ^b	C _t –C _c –C _t	L–Pd–L ^c	H _a –C _t –C _c –C _t	H _s –C _t –C _c –C _t
1	C _s		2.174 2.16 ^d	2.160 2.15 ^d	1.426		114.6		33.6	–165.2
2	C _s	F [–]	2.086	2.032	1.438	2.097	114.6	96.2	38.5	–165.4
3	C _s	Cl [–]	2.123	2.075	1.432	2.445	115.8	103.5	35.4	–166.3
4	C _s	NH ₃	2.157	2.137	1.424	2.229	116.3	96.0	34.8	–168.7
5	C _t	CH ₂ =CH ₂	2.198	2.205	1.419	2.214	117.3	104.2	30.7	–171.6
6	C _s	PH ₃	2.212	2.192	1.422	2.392	118.3	103.5	31.3	–171.4

^a Distances in Å and angles in deg. ^b NPd (**4**), PPd (**6**), and (CC)Pd, where (CC) is the midpoint of the C=C bond. ^c NPdN (**4**), (CC)Pd(CC) (**5**), and PPdP (**6**). ^d MCPDF/DZ+P results from ref 36.

Table 2. Calculated Complexation Energies of Molecules 1–6^a

L	MP2/A// MP2/A	MP2/B// MP2/A	MP3/B// MP2/A	MP4SDQ/B// MP2/A
1	0	0	0	0
2 F [–]	–207.6	–207.7	–208.8	–209.5
3 Cl [–]	–188.5	–191.3	–182.5	–186.4
4 NH ₃	–85.6	–88.7	–84.6	–84.9
5 CH ₂ =CH ₂	–70.4	–79.1	–57.9	–64.2
6 PH ₃	–80.2	–91.7	–74.6	–79.7

^a See eq 1. All energies in kcal/mol.

by these methods,^{67,68} at least for compounds of the second and third transition-metal row. Accordingly, in this section the calculated relative stabilities of the (η^3 -allyl)PdL₂ complexes will be analyzed by comparison of the complexation energies (Table 2) obtained from eq 1.

$$\Delta E_{\text{complexation}} = E[(\eta^3\text{-allyl})\text{PdL}_2] - [E(\mathbf{1}) + 2E(\text{L})] \quad (1)$$

Since the electrostatic attraction between the positively charged **1** and negatively charged ligands (F[–] and Cl[–]) is much stronger than this interaction with neutral ligands (NH₃, PH₃ and CH₂=CH₂), $\Delta E_{\text{complexation}}$ is larger by about 100 kcal/mol for anionic complexes **2–3** than for cationic complexes **4–6**.

For anionic σ -donors the ligand electronegativity has a large influence on the complexation energies. Thus, complexation of **1** with F[–] ions is more exothermic by 23 kcal/mol than with Cl[–] ions. In the case of neutral ligands, complexation with the σ -donor NH₃ is the most exothermic. Although the η^3 -allyl moiety is much more weakly bonded in **4** than in **6**, complexation energies for L = NH₃ (–84.9 kcal/mol) and L = PH₃ (–79.7 kcal/mol) differ only by 5 kcal/mol. π -Acceptors apparently weaken the Pd–C bonds; however, the concomitant thermodynamic destabilization is compensated by the π -back-bonding from the metal. The palladium–carbon distances are nearly the same in **5** and **6**; nevertheless, **1** is more stabilized when it coordinates with PH₃ (**6**) than with CH₂=CH₂ (**5**), suggesting that stabilization by π -back-bonding is more effective in the former case. Hay,⁵⁹ as well as Bäckvall and co-workers,⁶⁰ extensively discussed the surprisingly weak back-bonding interactions between CH₂=CH₂ and palladium.

Mulliken Population Analysis. Because of the well-known dependence of Mulliken charges on the basis set and computational level,⁶⁹ the discussion of this

Table 3. Mulliken Charges Calculated from the MP2/A Response Density^a

L	q _{total}	q(C _t)	q(C _c)	q(C _t H ₂)	q(C _c H)	q(allyl)
1	1.000	–0.507	–0.074	0.130	0.252	0.512
2 F [–]	–1.000	–0.516	–0.180	–0.023	0.051	0.005
3 Cl [–]	–1.000	–0.549	–0.182	–0.033	0.058	–0.008
4 NH ₃	1.000	–0.518	–0.097	0.062	0.194	0.318
5 CH ₂ =CH ₂	1.000	–0.514	–0.052	0.097	0.248	0.450
6 PH ₃	1.000	–0.518	–0.071	0.078	0.223	0.379

^a Charges in electron.

Table 4. Bond Critical Points (r_b) Evaluated from the MP2/A Response Density^a

L	interatomic regions					
	Pd–C _t		Pd–C _c		C _t –C _c	
	$\rho(\mathbf{r}_b)$	$H(\mathbf{r}_b)$	$\rho(\mathbf{r}_b)$	$H(\mathbf{r}_b)$	$\rho(\mathbf{r}_b)$	$H(\mathbf{r}_b)$
1	0.72	–0.26	0.71	–0.25	1.97	–2.11
2 F [–]	0.89	–0.44	0.97	–0.55	1.89	–1.96
3 Cl [–]	0.81	–0.35	0.87	–0.43	1.92	–2.01
4 NH ₃	0.76	–0.30	0.75	–0.29	1.97	–2.10
5 CH ₂ =CH ₂	0.68	–0.23	0.64	–0.19	1.98	–2.13
6 PH ₃	0.67	–0.21	0.66	–0.21	1.97	–2.12

^a $\rho(\mathbf{r}_b)$ in e/Å³ and $H(\mathbf{r}_b)$ in hartree/Å³.

section is restricted to a few typical changes of atomic and group charges, which can be ascribed to the ligand effects. Inspection of the data in Table 3 reveals that complexation of **1** with various ligands leads to (i) accumulation of the charge density at C_t and (in the case of σ -donor ligands) at C_c as well, (ii) a similar change of the group charges at C_cH and at the two C_tH₂ units, and (iii) charge transfer from PdL₂ to the η^3 -allyl moiety. According to the Mulliken analysis the η^3 -allyl moiety in the anionic complexes is neutral, while in the cationic complexes it has some allyl cation character. Yet, 60–70% of the positive charge in the cationic complexes is concentrated in the PdL₂ unit. This is in line with the observation of Malet and co-workers,⁷⁰ which suggests that the positive charge density in [(η^3 -arylallyl)Pd(dppe)]⁺ complexes is localized mainly in the PPdP region.

Bond Analysis. Analysis of the electron density distribution $\rho(\mathbf{r})$ in the palladium–carbon regions (Table 4) reveals that there are covalent bonds connecting Pd–C_t and Pd–C_c. Recognition of the covalent character of the palladium–carbon bonds is of relevance for the correct description of the orbital interactions in (η^3 -allyl)PdL₂ complexes. Covalent palladium–carbon bonding implies that, instead of ionic, electrostatic, or other closed-shell interactions, the three palladium–carbon bonds are formed by orbital overlap between the corresponding MOs of the allyl fragment and the metal. In addition, the electron density $\rho(\mathbf{r}_b)$ and energy density

(67) Yoshida, T.; Koga, N.; Morokuma, K. *Organometallics* **1995**, *14*, 746.

(68) Dapprich, S.; Pidun, U.; Ehlers, A. W.; Frenking, G. *Chem. Phys. Lett.* **1995**, *242*, 521.

(69) Hehre, W. J.; Radom, L.; Schleyer, P. v. R.; Pople, J. A. *Ab Initio Molecular Orbital Theory*; Wiley: New York, 1986.

(70) Malet, R.; Moreno-Mañas, M.; Parella, T.; Pleixats, R. *Organometallics* **1995**, *14*, 2463.

$H(\mathbf{r}_b)$ in the bond critical point of Pd–C_c and Pd–C_t are rather similar, suggesting that the bond to the central carbon is about as strong as one of the bonds to a terminal carbon. This is in line with the observation of Kozhevina and Yurchenko,^{71,72} which shows that the harmonic force constants of the Pd–C_c and Pd–C_t coordinates are similar. Using the experimental IR spectrum of $[(\eta^3\text{-allyl})\text{PdCl}]_2$, these authors calculated values of 1.29 and 1.15 mdyn/Å for $k_{\text{Pd-C}_c}$ and for $k_{\text{Pd-C}_t}$, respectively.⁷¹

The $\rho(\mathbf{r}_b)$ and $H(\mathbf{r}_b)$ values correlate well with the palladium–carbon bond lengths. Thus, the electron density in the Pd–C regions is high when L is a σ -donor, and it is low when L is a π -acceptor. Complexation of **1** with pure σ -donors always increases the electron density in Pd–C regions, while complexation with π -acceptors has the opposite effect. As one goes from **2** to **6**, $\rho(\mathbf{r}_b)$ of Pd–C is reduced by 30%, which also implies a substantial decrease of the palladium–carbon bond orders.⁵¹ This also explains why π -acceptors but not σ -donors activate $(\eta^3\text{-allyl})\text{PdL}_2$ complexes toward nucleophilic attack. A nucleophilic attack involves breaking of the palladium–carbon bond, which is easier in those complexes where the carbon atom is more weakly bonded to Pd.

A small but significant change of $\rho(\mathbf{r}_b)$ and $H(\mathbf{r}_b)$ can be observed in the C_t–C_c bond critical point. Increase of $\rho(\mathbf{r}_b)$ and $H(\mathbf{r}_b)$ in the Pd–C bond critical points is accompanied by a decrease of $\rho(\mathbf{r}_b)$ and $H(\mathbf{r}_b)$ in the C_t–C_c bond critical points, suggesting that the electron density is pushed out of the C–C regions when the palladium–carbon interactions are strengthened. The magnitudes of the electron densities in Pd–C regions, which strongly depend on the ligand, have a large influence on the hyperconjugative ability of the Pd–C bonds. There are clear indications that charge transfer from Pd–C bonds to low-lying σ^* orbitals of allylic β -substituents leads to asymmetric allyl–Pd bonding, which governs the chemo-, regio-, and stereoselectivity of the nucleophilic attack.⁷³

4. Extension of the *ab Initio* Results to Other Ligands. Effects of σ -Donors/ π -Acceptors on the Reactivity and Regioselectivity in Nucleophilic Additions

Elucidation of the ligand effects for other, more commonly employed ligands requires a deeper understanding of the orbital interactions in the $(\eta^3\text{-allyl})\text{PdL}_2$ complexes. In this connection, the following questions have to be considered. (1) Why is the more electronegative F[−] a better σ -donor than Cl[−]? (2) Why do σ -donors strengthen and π -acceptors weaken the palladium–carbon bonds? (3) How do the frontal orbital levels depend on the nature of the ligand? (4) How are substitution and chelation expected to change the ligand effects of NH₃, CH₂=CH₂ and PH₃?

Further interpretation of the computational results will be given by means of an MO diagram that summarizes the major orbital interactions between the allyl fragment and PdL₂. Curtis and Eisenstein³⁸ (CE) have

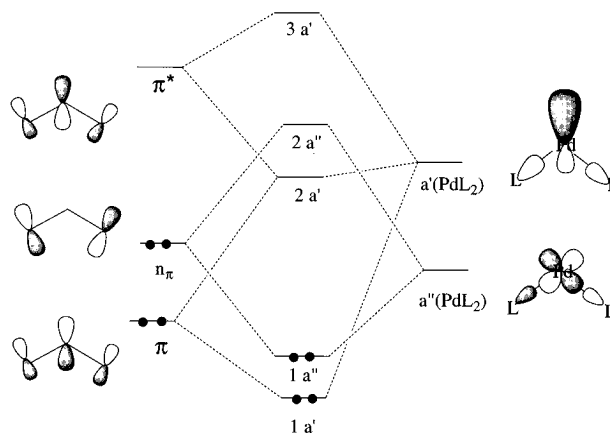


Figure 2. Orbital interaction diagram for $(\eta^3\text{-allyl})\text{PdL}_2$.

presented an energy level diagram that describes palladium–carbon bonding in $[(\eta^3\text{-allyl})\text{PdCl}_2]^-$ by interactions of the free allylic n_π and $4d_{xz}(\text{Pd})$ MOs. However, in a recent publication Carfagna and co-workers⁴⁰ argued against this description, pointing out that the distortion of the complexed η^3 -allyl moiety has to be explicitly considered. It was shown⁴⁰ that the $\pi^*(\text{allyl})$ level is considerably stabilized, while $\pi(\text{allyl})$ is slightly destabilized, by distortion of the free allyl species.

The MO description given by CE implies that only C_t atoms are covalently bonded to Pd. However, the bond analyses (*vide supra*) showed that C_c is covalently bonded as well. Therefore, in an improved MO diagram orbital overlap between π and π^* FMOs of the distorted allyl moiety, which have large amplitudes on C_c, and a PdL₂ FMO of the same symmetry also have to be considered. Accordingly, a qualitative orbital interaction diagram (Figure 2) was constructed by assuming C_s symmetry for the $(\eta^3\text{-allyl})\text{PdL}_2$ complex. This MO diagram is assembled from allylic fragment orbitals π , n_π , and π^* of the complexed allyl anion and two fragment orbitals of PdL₂ (L = σ -donor), which possess a' and a'' symmetries (for derivation of these fragment orbitals see, e.g., ref 74). FMOs a''(PdL₂) and a'(PdL₂) are made by an out-of-phase combination of $4d_{xz}-\sigma(\text{L}_2)$ and an in-phase combination of a $5sp(\text{Pd})\text{hybride}-\sigma(\text{L}_2)$ MOs, respectively.⁷⁴ The block of d(Pd) orbitals and other combinations of d(Pd)– $\sigma(\text{L}_2)$ orbitals accommodating a total of 12 electrons are not displayed in Figure 2, since these orbitals are not expected to give significant contribution to the Pd–C_c bonding.^{38,40} The a''(PdL₂) orbital interacts with $n_\pi(\text{allyl})$, yielding filled $1a''$ Pd–C_t bonding and empty $2a''$ Pd–C_t antibonding MOs. The a'(PdL₂) orbital overlaps in a σ fashion with $\pi(\text{allyl})$ and $\pi^*(\text{allyl})$ fragment orbitals. An in-phase combination of the filled $\pi(\text{allyl})$ with the empty a'(PdL₂) leads to Pd–C_c bonding. Since $\pi(\text{allyl})$ is carbon–carbon bonding, this interaction weakens the C_t–C_c bond compared to free allyl species. Furthermore, second-order mixing of $\pi^*(\text{allyl})$ with $\pi(\text{allyl})$ also decreases C_t–C_c bonding. These effects are clearly reflected in the calculated geometrical parameters and bond analysis data. (1) C_t–C_c in free allyl species (1.37–1.39 Å,⁶² HF/6–31G*, HF/6–31+G*) is shorter by 0.03–0.07 Å than in $(\eta^3\text{-allyl})\text{PdL}_2$ complexes (1.42–1.44 Å). (2) Ligand effects that lead to shortening of Pd–C_c are accompanied by

(71) Kozhevina, L. I.; Yurchenko, E. N. *Zh. Prikl. Spektrosk.* **1974**, *21*, 291.

(72) Kozhevina, L. I.; Yurchenko, E. N. *Zh. Prikl. Spektrosk.* **1976**, *24*, 161.

(73) Szabo, K. J. Unpublished results.

(74) Albright, T. A.; Burdett, J. K.; Whangbo, M.-H. *Orbital Interactions in Chemistry*; Wiley: New York, 1985, Chapters 1 and 19.

lengthening of C_c–C_t (Table 1). (3) An increase of electron density in the Pd–C_c bond critical point leads to a decrease of electron density in C_t–C_c bond critical points (Table 4).

The σ -Donor ability of L is expected to have a greater influence on the a''(PdL₂) energy level than on the a'(PdL₂) energy level, since the out-of-phase s–d–s overlap in a''(PdL₂) is close to the optimal 90°, while the in-phase s–p–s overlap in a'(PdL₂) is rather poor.⁷⁴ Accordingly, strong σ -donors will raise and slightly lower the a''(PdL₂) and a'(PdL₂) levels, respectively. Strengthening of Pd–C bonding by increasing the electronegativity of L can be explained by the presumably small energy gap between the low-lying σ levels of electronegative ligands and 4d levels of Pd(II). Ziegler and co-workers⁷⁵ have shown that the average energy of valence orbitals of Pd, compared to other transition metals, is relatively low. Lowering the energy of σ (L₂) causes the energy gap between a''(PdL₂) and n_τ to diminish. Consequently, there will be stronger Pd–C_t interactions, since 1a'' is stabilized. Coordination of π -acceptors involves charge transfer from the metal to the ligand through back-donation that leads to orbital contraction and, therefore, further lowering of the 4d levels. Consequently, 1a'' is destabilized and the 1a''–2a'' splitting is reduced. Weakening of Pd–C_t bonding and lowering of the unfilled 2a'', which is Pd–C_t antibonding, leads to activation of the allyl moiety toward nucleophilic attack. As was mentioned above, this activation does not necessarily mean a considerable decrease of the thermodynamic stability of the complex. Therefore, (η^3 -allyl)PdL₂ complexes, with σ -donor ligands (e.g. Cl[–], OAc[–], tmeda, etc.) can be easily activated by exothermic or slightly endothermic ligand exchange to π -acceptors (phosphines, phosphites, benzoquinone, etc.). Since the palladium-carbon bonds in unligated **1** are also weaker than in **2–4**, very weak σ -donors such as solvent molecules are also able to activate (η^3 -allyl)PdL₂ toward nucleophilic attack.

Variation of the relative positions of 2a' and 2a'' on changing of the ligand affects the regiochemistry of the nucleophilic attack. If 2a'' is the LUMO, terminal attack is expected, since 2a'' has large amplitudes at the terminal carbons. However, if the energies of the two low-lying virtual MOs are switched and 2a' becomes the LUMO, central attack occurs, since this orbital has larger MO coefficients at the central carbon than at the terminal carbons of the allyl ligand. Calculations at the HF/A level of theory show that, for example, in **4** (L =

NH₃) 2a' is the LUMO 0.4 eV below 2a'', while in **1** the order is reversed and 2a'' is the LUMO and the energy difference between the two levels is 0.8 eV.

The most commonly used ligands are substituted derivatives of NH₃, CH₂=CH₂, and PH₃. Electron-donating substituents such as alkyl groups will increase the σ -donor strength of these ligands. Therefore, in (η^3 -allyl)PdL₂ complexes, where L = NR₃, CR₂=CR₂, and PR₃, stronger and shorter palladium-carbon bonds are expected than in **4–6**. Electron-withdrawing substituents, which are often applied in phosphines and phosphites, will amplify the π -acceptor character⁷⁶ of the ligands that weaken the palladium-carbon bonds and activate the complexes. Chelation by bidentate ligands changes the L–Pd–L angle. For example, in [(η^3 -allyl)Pd(tmeda)]⁺ and [(CH₃)₂Pd(tmeda)]⁺ complexes the N–Pd–N bite angles are 84.6(5)⁵⁷ and 82.73(8)⁷⁷ respectively, which are smaller by 12–14° than N–Pd–N in **4** (96.0°). The P–Pd–P bite angle in the [(CH₃)₂Pd(dmpe)]⁺ complex (85.4°) is considerably smaller than the corresponding parameter in **6** (103.5°). A relatively small decrease in L–Pd–L angle is expected to stabilize 2a' to a somewhat larger extent than 2a'', because in the region 80° < L–Pd–L < 100° the angular dependence of the s–p–s overlap is stronger than that of the s–d–s overlap⁷⁴ and, therefore, chelation will increase the probability of central attack by nucleophiles. This is line with the experimental findings that tmeda and, to a lesser extent, bppe ligands direct nucleophilic attack at C_c of (η^3 -allyl)PdL₂ complexes.^{11–13,23}

Acknowledgment. This work was supported by the Swedish Natural Science Research Council (NFR). All calculations were done on the Cray Y-MP8D/464 of the Nationellt Superdatorcentrum (NSC), Linköping, Sweden. I thank the NSC for a generous allotment of computer time. I am grateful to Prof. Dieter Cremer and Dr. Elfi Kraka (University of Gothenburg, Gothenburg, Sweden) for granting access to their density analysis program.

Supporting Information Available: Tables and figures giving calculated geometries and locations of bond critical points for structures **1–6** (6 pages). Ordering information is given on any current masthead page.

OM950715O

(76) Rahman, M. M.; Liu, H.-Y.; Eriks, K.; Prock, A.; Giering, W. P. *Organometallics* **1989**, *8*, 1.

(77) de Graaf, W.; Boersma, J.; Smeets, W. J. J.; Spek, A. L.; van Koten, G. *Organometallics* **1989**, *8*, 2907.

(75) Ziegler, T.; Tschinke, V.; Ursenbach, C. *J. Am. Chem. Soc.* **1987**, *109*, 4825.